ISSN 1068-3356, Bulletin of the Lebedev Physics Institute, 2024, Vol. 51, Suppl. 7, pp. S543–S556. © Allerton Press, Inc., 2024.
Russian Text © The Author(s), 2024, published in Kvantovaya Elektronika, 2024, Vol. 54, No. 3, pp. 137–145.

INTERACTION OF LASER RADIATION WITH MATTER

Increased Nuclear Reaction Yields in Cluster Targets Irradiated with Circularly Polarized, Short and Intense Laser Pulses

A. A. Andreev[a,b], L. A. Litvinov[a], and K. Yu. Platonov[c,*]

[a] *St. Petersburg State University, St. Petersburg, 190034 Russia*
[b] *Ioffe Institute of Physics and Technology, St. Petersburg, 194021 Russia*
[c] *Peter the Great St. Petersburg Polytechnic University, St. Petersburg, 195251 Russia*
**e-mail: konstantin_platonov@yahoo.com*

Received April 20, 2024; revised June 3, 2024; accepted June 3, 2024

Abstract—Analytical estimates and numerical simulation were used to review the yield of nuclear reaction products in a separate cluster and in the focal volume of laser cluster plasma. The circular polarization of a short intense laser pulse is shown to produce an average magnetic field that keeps the plasma of the focal volume from transverse expansion. An extension of plasma lifetime results under certain conditions in a significant (up to double) increase in neutron yield in the Li$(D, n)^8$Be reaction compared to plasma heating by a linear polarization laser pulse when the magnetic field is absent.

Keywords: circularly polarized ultrashort laser pulse, laser cluster plasma, strong quasi-stationary magnetic field, nuclear reaction

DOI: 10.3103/S1068335624601754

1. INTRODUCTION

It is well known that submicron diameter clusters interacting with an intense and ultrashort laser pulse heat, ionize and scatter coulombically or thermally generating high-energy charged particles [1]. With an appropriate choice of laser parameters and of the composition, size, and density profile of the target, the generated ions can reach high energies sufficient to initiate nuclear reactions [2].

Recent theoretical studies and numerical simulation have predicted that, for example, nuclear fusion is also possible within a single cluster in collisions between ions as a result of a Coulomb explosion [3, 4]. The yield of the reaction between particles (the number of reaction acts) in a spherical expanding cluster depends on the cluster expansion rate because, as the cluster radius increases, the adiabatic temperature/energy of reacting particles drops and their density decreases, which terminates nuclear reactions. The small focal volume of the laser pulse and rapid expansion of the cluster laser plasma produce few reaction acts, so there arises the task to optimize the parameters of the laser and of the cluster target in order to increase the yield of reaction products.

We propose in this paper a method to increase the lifetime of cluster laser plasma by means of circular polarization of the plasma-generating laser pulse. An intense orbital electron current is known to arise in this case around clusters, which generates a quasi-stationary magnetic field comparable to the laser field in amplitude [5–7]. The superstrong magnetic field slows down the transverse expansion of both individual clusters and of the entire focal volume of laser plasma increasing several times the lifetime of the cluster plasma magnetized in the focal volume of the laser pulse, which should increase the yield of nuclear reaction products. An additional advantage of the laser cluster target is the possibility to use frequency lasers [8] that repeat the laser pulse with a frequency of 1 Hz or higher thus making it possible to create a quasi-stationary source of nuclear reaction products, for instance a neutron source although in this case there are limitations on the laser pulse energy.

2. DETERMINING THE NUMBER OF NUCLEAR REACTIONS IN CLUSTER PLASMA

Consider first a homogeneous dense plasma cluster consisting of atoms of two types, N_a and N_b, and irradiated by an intense circularly polarized laser pulse. Nuclear reactions are known to be possible in this case as a result of heating, scattering and collisions of ions [9]. The reaction yield is determined by integrals

over the distribution functions of reacting particles (distribution function moments). When normalized to the total number of particles N_a, N_b, the distribution function moments of different functional form differ from each other by a multiplier of the order of one. Accordingly, to estimate the reaction yield with such accuracy, the distribution functions of ions of a and b type involved in the nuclear reaction in the hydrodynamic approximation as $f_{a,b}(r, v, t) = n_{a,b}(r, t) \cdot \delta(v - v_{a,b}(r, t)e_r)$. Then the yield of reaction products with spherically symmetric expansion is estimated through the reaction cross section σ_{ab} as [4]

$$N = \int f_a(r,v_a,t) f_b(r,v_b,t) \sigma_{ab}\left(\frac{m_{ab}(v_a - v_b)^2}{2}\right) \times |v_a - v_b| d^3v_a d^3v_b dt dV = \int_0^\infty dt \int_0^{R(t)} n_a(r,t) n_b(r,t) \times \sigma_{ab}\left(\frac{m_{ab}(v_a(r,t) - v_b(r,t))^2}{2}\right)[v_a(r,t) - v_b(r,t)] 4\pi r^2 dr, \quad (1)$$

where m_{ab} is the reduced mass of ions. The hydrodynamic densities included in (1), $n_{a,b}(r, t)$, and radial velocities, $v_{a,b}(r,t)$ are taken from the system of hydrodynamic equations describing the thermal [10] or Coulomb [11] cluster expansion.

2.1. Analytical Estimates

To estimate the integral (1) by the order of magnitude, an approximate solution to the set of hydrodynamic equations is sufficient, where the profiles of the densities, $n_{a,b}(r, t)$ maintain a rectangular form throughout the expansion:

$$n_{a,b}(r,t) = \frac{\theta(R_{a,b}(r) - r) 3N_{a,b}}{4\pi R_{a,b}^3(t)}, \quad v_{a,b}(r,t) = \frac{r\dot{R}_{a,b}(t)}{R_{a,b}(t)}. \quad (2)$$

Here $\theta(x)$ is the stepped Heaviside function; $R_{a,b}(t)$ are the outer density front radii of a, b ions; $v_{a,b}(r,t)$ are the radial components of the hydrodynamic velocity of ions. Note that the replacement of the rectangular density profile by a parabolic one (stepped in [12]) leads to a multiplier of the order of one in the integral (1), i.e., accuracy is the same as in using the distribution function in hydrodynamic approximation. Consider a ions as heavy and b ions as light, the ratio of the ion charge to its mass being $Z_a/m_a < Z_b/m_b$, $v_a(r,t) < v_b(r,t)$.

The approximate solution to (2) does not take into account the effects of interaction between the fronts of light and heavy ions [13], of front breaking, and of the multistream flow of light ions [14] because such effects involve a small number of cluster ions compared to N_a, N_b, and we can consider the expansion of light and heavy ion components independently. Numerical PIC simulation of the cluster expansion with ions of two types under the action of a laser pulse [15] also demonstrates the presence of two expanding spherical fronts when the light ion front outpaces the heavy ion front.

We substitute the densities $n_{a,b}(r, t)$ and velocities $v_{a,b}(r,t)$ (2) into (1). The integral over r in (1) is other than zero only for $0 < r < R_a(t) \le R_b(t)$ (light b ions are ahead of heavy a ions), then N is estimated as

$$N = \frac{9N_aN_b}{16\pi^2}\int_0^\infty dt \frac{1}{R_a^3(t)R_b^3(t)} \int_0^{R_a(t)} \sigma_{ab}\left\{\frac{m_{ab}r^2}{2}\left[\frac{\dot{R}_a(t)}{R_a(t)} - \frac{\dot{R}_b(t)}{R_b(t)}\right]^2\right\} \times \left\{r\left[\frac{\dot{R}_a(t)}{R_a(t)} - \frac{\dot{R}_b(t)}{R_b(t)}\right]\right\} 4\pi r^2 dr \approx \frac{9N_aN_b}{16\pi}\int_0^\infty dt \frac{1}{R_b^3(t)} \times \sigma_{ab}\left\{\frac{m_{ab}}{2}\left[\dot{R}_a(t) - \frac{\dot{R}_b(t)R_a(t)}{R_b(t)}\right]^2\right\}\left[\dot{R}_a(t) - \frac{\dot{R}_b(t)R_a(t)}{R_b(t)}\right]. \quad (3)$$

We consider reactions in which the σ_{ab} cross section is maximum in the mega-electron-volt range of ion energies. The path of light ions with energy ~10^6 eV in a target with density $n_a \sim 10^{22}$ cm^{-3} exceeds tens

of micrometers. The initial radii of clusters are hundreds of nanometers, so we neglect the ion energy losses and finite path length when considering the single cluster expansion.

2.2. Cluster Plasma without Magnetic Field

Consider first the process without a magnetic field. The law of conservation of energy (the integral of the equation of motion of ion scattering at the outer boundary of the cluster) under the action of thermal and Coulomb forces has the following form:

$$\frac{m_{a,b}}{2}\left(\frac{dR_{a,b}(t)}{dt}\right)^2 + \frac{3Z_{a,b}R_{\text{eh}}(1-k)R_0^2}{R_{a,b}^2(t)} + \frac{Z_{a,b}eQ}{R_{a,b}(t)} = 3Z_{a,b}T_{\text{eh}}(1-k) + \frac{Z_{a,b}eQ}{R_0}. \quad (4)$$

In (4) $T_{\text{eh}} \approx m_e c^2(I\lambda^2/1.37\times 10^{18})^{\mu}$, $0.5 \le \mu \le 1$ is the temperature of hot cluster electrons [16] accelerated by a circularly polarized laser pulse with intensity I; Q is the total electric charge acquired by the cluster due to the removal of electrons by the laser field; $k = 3Q/[4\pi e(Z_a n_{a0} + Z_b n_{b0})R_0^3]$ is a dimensionless charge of the cluster in units of its maximum possible value of $4\pi e(Z_a n_{a0} + Z_b n_{b0})R_0^3/3$. The numerical simulation below showed that $\mu \approx 0.75$ for the cluster plasma and circular polarization of the laser pulse. The power exponent $\mu \approx 0.75$ occupies an intermediate position between solid-state targets ($\mu \approx 0.5$) [17] and free electrons ($\mu \approx 1$).

For the electrons to be confined by the ion skeleton of the cluster resulting from partial extraction of electrons by the main laser pulse, the cluster charge Q must satisfy the inequality $T_{\text{eh}} < eQ/(CR_0)$ (the kinetic energy of an electron is less than the potential energy); accordingly, to estimate the cluster charge, we get the expression $Q \approx CT_{\text{eh}}R_0/e$ where the numerical factor $C \sim 1$ and Q grows with increasing laser intensity as I^{μ} and cannot exceed the total charge of the cluster's ion skeleton $4\pi e(Z_a n_{a0} + Z_b n_{b0})R_0^3/3$. The parametric solution of Eq. (4) is written as

$$\begin{aligned} R_{a,b}(\xi) &= R_0\left(\frac{\kappa}{2} + \left(1-\frac{\kappa}{2}\right)\cosh\xi\right), \quad \xi \in [0;\infty], \\ t(\xi) &= \frac{R_0}{\sqrt{2Z_{a,b}W/m_{a,b}}}\left[\left(1-\frac{\kappa}{2}\right)\sinh\xi + \frac{\kappa\xi}{2}\right], \\ W &= 3T_{\text{eh}}(1-k) + \frac{eQ}{R_0}, \quad \kappa = \frac{eQ}{WR_0}. \end{aligned} \quad (5)$$

The parameter $0 \le \kappa \le 1$ in (5) is responsible for the relation between the Coulomb and thermal forces that accelerate the outer boundary of the cluster. It is convenient to use for practical estimates of the dependence of the heavy and light ion scattering radii $R_{a,b}(t)$ on time in the interval $R_0 \le R_{a,b}(t) \le 10R_0$ ($R_{a,b}(t=0) = R_0$), a simple approximation (5) taking into account the scattering of cluster ions under the action of thermal and Coulomb forces as follows:

$$R_{a,b}(t) \approx \sqrt{R_0^2 + 2(1-0.3\kappa)Z_{a,b}Wt^2/m_{a,b}}. \quad (6)$$

An estimate follows from (6) of characteristic scattering velocities of the heavy a and light b ion components of the cluster, $\dot{R}_{a,b}(t\to\infty) \approx \sqrt{2(1-0.3\kappa)Z_{a,b}W/m_{a,b}}$. When substituting (6) into (3), the estimate N takes the form:

$$\begin{aligned} N &\approx \frac{3N_aN_b}{16\pi R_0^2}\sigma_{ab}(\varepsilon^*)\frac{\chi^2+\chi-\chi}{\chi(\chi+1)}, \quad \chi = \sqrt{\frac{Z_b m_a}{Z_a m_b}} \ge 1, \\ \varepsilon^* &= (1-0.3\kappa)W\left(\sqrt{\frac{Z_b m_{ab}}{m_b}} - \sqrt{\frac{Z_a m_{ab}}{m_a}}\right)^2. \end{aligned} \quad (7)$$

It is convenient to use as a target substance for clusters a saturated solution of LiF salt in heavy water (reaction Li + D = ^{8}Be + n). The cross section of this reaction $\sigma_{\text{DLi}}(\varepsilon_{\text{D}}\,[\text{MeV}]) = (1.9\times 10^{-22}/\varepsilon_{\text{D}})\exp(-6\varepsilon_{\text{D}}^{-0.4})$ [cm^2] remains large (~1 barn) for ε_{D} energies in the range of 1 to 100 MeV [18]. The density is ~10^{22} cm^{-3} for this solution and the number of particles $N_{\text{Li, D}} \approx 1.3\times 10^8$ for the cluster radius $R_0 = 100$ nm. The characteristic energy ε^* of the relative motion of Li and D ions coincides with the cross section maximum: $\varepsilon^* = 2$ MeV for $I \approx 2\times 10^{20}$ W/cm^2 and $Z_{\text{Li}}/A_{\text{Li}} = 3/7$, $Z_{\text{D}}/A_{\text{D}} = 1/2$. The reaction yield N for a single cluster is ~1 neu-

tron. In addition to this reaction, neutrons are also generated by the collision of deuterium nuclei, where the cross section $\sigma_{DD}(\varepsilon_D) = 7.32 \times 10^{-24}\varepsilon_D^{-1} \times \exp(-4.33\varepsilon_D^{-0.285})$ [cm^2] in the MeV deuteron energy range is an order of magnitude smaller and the DD channel contribution is small at high laser intensities. However, at deuteron energies less than 400 keV (low laser intensities [19]), the cross section of the D–D reaction will exceed that of the Li–D reaction and the DD channel will be determinant.

As it is known, the longitudinal dimension of the focal region is $\sim\pi D^2/(2\lambda)$ for the laser pulse focus spot diameter D, i.e., it is approximately twice the Rayleigh length. Let $s > 2R_0$ be the characteristic distance between the cluster centers in the cluster plasma, then the cluster concentration $n_{cl} \approx s^{-3}$ and the total number of clusters in the focal volume $N_{cl} \approx \pi^2 D^4/(8\lambda s^3)$. The minimum possible value of $s \approx 4R_0$ is a practically realizable case when the distance between clusters is of the order of the cluster diameter and the clusters do not merge. When clusters expand apart in the focal volume, nuclear reactions occur not only in each of the clusters, but also at the collision of ions belonging to different clusters. As a result, the total neutron yield N_{tot} from the focal volume is determined by the sum of two summands:

$$N_{tot} = N_{in} + N_{out} \approx NN_{cl} + \frac{2N_aN_bN_{cl}(N_{cl}-1)\lambda}{\pi^2 D^3} \times \sigma_{ab}[(1-0.3\kappa)W(Z_b+Z_a)], \quad (8)$$

where $N_{in} = NN_{cl}$ is the number of within clusters and N_{out} ix the number of inter cluster reactions.

The change in the argument of the cross-section in the second summand of (8) is due to the change in the relative velocity square $\overline{v}_{rel}^2 = (\overline{v}_b - \overline{v}_a)^2$, which is part of the cross-section argument in (1) for ions of different clusters, and the averaging over the angles between the velocities leads to $\langle\overline{v}_{rel}^2\rangle = \langle\overline{v}_b^2\rangle + \langle\overline{v}_a^2\rangle$ wherefrom the sum $Z_b + Z_a$ appears in (8). The ratio of the two summands in (8) determines which type of collisions (within or between clusters) is the main input into N_{tot}:

$$\frac{N_{in}}{N_{out}} \approx \frac{3s^3(\chi^2+\chi-2)}{4R_0^2D\chi(\chi+1)} \frac{\sigma_{ab}(\varepsilon^*)}{\sigma_{ab}[(1-0.3\kappa)W(Z_b+Z_a)]}. \quad (9)$$

For example, the focal volume is 10^4 μm^3 for $D = 10$ μm. At a distance of $s = 1$ μm between clusters with $R_0 = 100$ nm, the total neutron yield from the focal volume is approximately 2.5×10^4 neutrons at intensity $I \approx 2 \times 10^{20}$ W/cm^2 for a 10 femtosecond laser pulse, and for these parameters $N_{in} \sim N_{out}$.

2.3. The Results of Numerical Simulation

To verify the above estimates, numerical PIC simulation of the laser cluster plasma was carried out using the EPOCH code [20]. Clusters with a radius of 250 nm were considered at the same concentration of 3×10^{22} cm^{-3} of Li_7^{3+} and D_3^{1+} ions. The distance between cluster centers s was 900 nm and the number of clusters was 27 ($3 \times 3 \times 3$). The simulation box of $x \times y \times z = 5 \times 3 \times 3$ μm was divided into $1000 \times 1000 \times 1000$ cells (spaced 5 nm), the central cluster being placed in the center of the box. A laser pulse of different intensities (10^{20} to 10^{22} W/cm^2) of 10 fs duration was focused on the central cluster, the focus spot diameter $D = 2.4$ μm for the wavelength $\lambda = 0.8$ μm. The O_{16}^{8+} and F_{19}^{9+} ions, which do not participate in the nuclear reaction, acted as ballast and may have caused energy losses of "working" Li_7^{3+} and D_2^{1+} ions in inelastic collisions of ions from neighboring clusters (elastic collisions did not affect the deuterium energy and nuclear reaction yield). However, estimates of the path length relative to inelastic collisions of D^{1+}, Li^{3+} ions with energies in MeV units in a medium with an average density of oxygen ions $\langle n_{iO}^{8+}\rangle = n_{cl}4\pi n_{i0}R_0^3/3$ and a characteristic concentration of clusters $n_{cl} \sim 1$ μm^{-3} give a value exceeding both the focal waist diameter D and the length of the focal region $\pi D^2/(4\lambda)$. Therefore, the O_{16}^{8+} and O_{19}^{9+} ions were disregarded in the numerical simulation in the EPOCH PIC code.

Figures 1, 2 show the numerical simulation data of the densities of Li and D cluster ions, the functions of energy distribution of electrons and of Li and D ions, and the dependence of the temperature T_{eh} of hot cluster electrons on laser intensity. Figures 1a, 1c shows the intense scattering of D^{1+} and Li^{3+} ions, density distributions being almost identical due to similar Z/A values. The average density values of D and Li ions on the color scales correspond to the average density $\langle n_D\rangle = n_{cl}4\pi n_{i0}R_0^3/3$ used in esti-

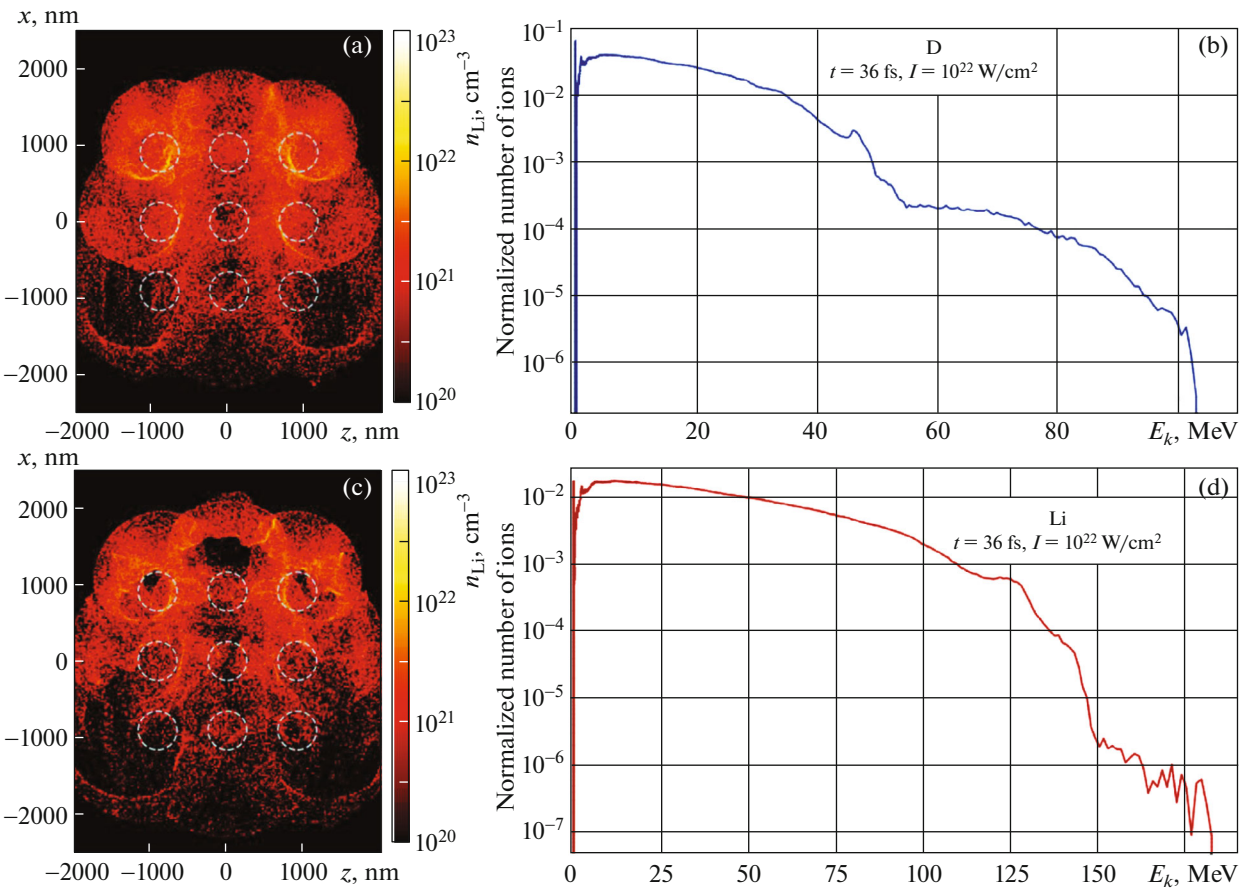

Fig. 1. Spatial distributions of deuterium and lithium ion concentrations of the cluster (a, c) and ion energy distribution functions at the end of laser pulse (t = 36 fs) (b, d). The blue curve indicates the boundaries of the ion distribution at the initial moment of time.

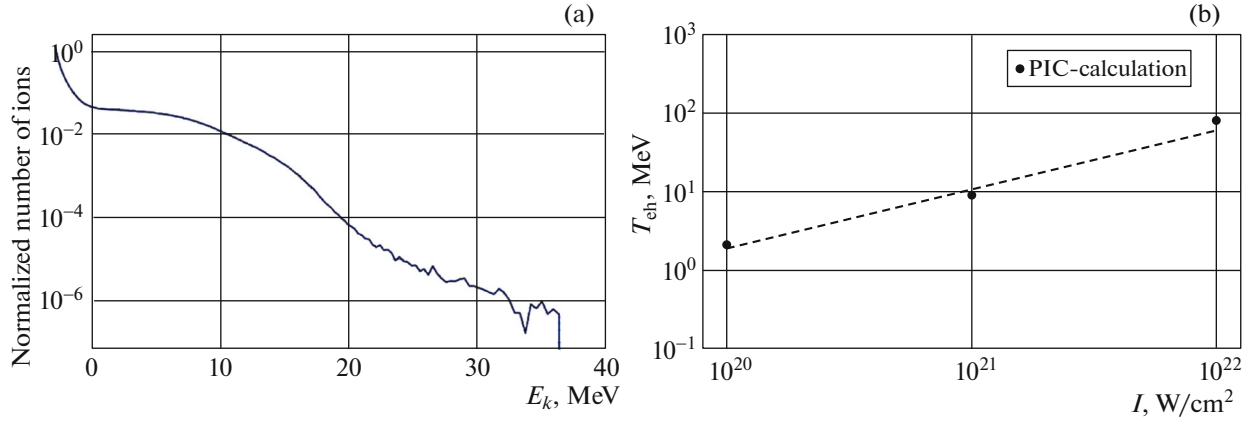

Fig. 2. Electron energy distribution function at the end of the laser pulse for the pulse intensity of 10^{21} W/cm^2, duration τ_{las} = 10 fs, λ_{las} = 0.8 μm, and the focus spot diameter $2w_0$ = 2.4 μm (a); and hot electron temperature T_{eh} obtained from electron distribution functions as laser intensity function (b). The approximation of T_{eh} dependence on intensity (shown by the dashed line) is $T_{eh} \propto I_{las}^{0.75}$ in the intensity range of 10^{20} to 10^{22} W/cm^2.

mates, where $n_{i0} = 3 \times 10^{22}$ cm^{-3} is the initial solid-state cluster density in the numerical simulation. Figures 1a, 1c also shows plasma acceleration by the ponderomotive pressure of the laser pulse in addition to isotropic scattering. There is a directional motion of ions along the x-axis of the laser pulse. The energies of accelerated ions in Figs. 1b, 1d and the energy of their relative motion $W(\sqrt{Z_b m_{ab}/m_b} - \sqrt{Z_a m_{ab}/m_a})^2$ fall

within the energy interval of the maximum cross section values of Li–D and D–D-reactions. The temperature dependence of hot electrons that accelerate ions (Fig. 2b) corresponds to the power scaling $T_{\text{eh}}\,[\text{MeV}] = 1.88 \times 10^{-15} \cdot I_{\text{las}}^{0.75}\,[\text{W/cm}^2]$.

When the radius of clusters is increased to several hundred nanometers in order to enhance the yield of reaction products, the Coulomb explosion of a cluster becomes impossible with currently achievable laser intensities. "Large" clusters expand based on a thermal mechanism (parameters $\kappa \to 0$, $k \to 0$), and in the case of a laser pulse with circular polarization an intense circular current of hot electrons appears around the cluster generating a longitudinal (along the laser beam axis) quasi-stationary magnetic field [5] comparable (superior under special conditions [6, 7]) to the laser field. The magnetic field breaks the spherical symmetry of the expansion and slows down the expansion in the transverse direction, which increases the effective interaction time of reacting nuclei (the effective interval of integration over time in (3)) and the yield of reaction products. Note that in the case of laser pulses of linear polarization, the magnetic field does not arise, and the estimates (3) and (8) are valid for clusters of "large" size. We consider below the effect of the magnetic field in more detail.

3. THE EFFECT OF THE MAGNETIC FIELD ON CLUSTER EXPANSION AND YIELD OF NUCLEAR REACTIONS

The magnetic field leads to anisotropy of the cluster expansion (the cluster acquires the shape of an ellipsoid of revolution) and to the appearance of two characteristic sizes $R_{\perp a,\,\perp b}(t)$, $R_{\|a,\,\|b}(t)$ instead of $R_{a,\,b}(t)$ as well as to the difference in expansion velocities along and across the field and to the appearance of the azimuthal component $v_{\varphi a,\varphi b}$ of ion velocities. The equations of the cluster dynamics in the magnetic field are given in Appendix 1.

The yield of reaction products (the formula similar to (3)) in the case of anisotropic cluster expansion takes the following form:

$$N = \frac{9N_aN_b}{16\pi^2}\int_0^\infty dt\,\frac{1}{R_{\perp a}^2(t)R_{\perp b}^2(t)R_{\|a}^2(t)R_{\|b}^2(t)}\int_0^{R_{\|a}(t)}dx\int_0^{R_{\perp a}(t)}\sigma_{ab}\left\{\frac{m_{ab}}{2}\left(r^2\left[\frac{\dot R_{\perp a}(t)}{R_{\perp a}(t)}-\frac{\dot R_{\perp b}(t)}{R_{\perp b}(t)}\right]^2\right.\right.$$
$$\left.+\frac{r^2}{4}\left[\Omega_a\left(\frac{R_{\perp 0}^2}{R_{\perp a}^2}-1\right)-\Omega_b\left(\frac{R_{\perp 0}^2}{R_{\perp b}^2}-1\right)\right]^2+x^2\left[\frac{\dot R_{\|a}(t)}{R_{\|a}(t)}-\frac{\dot R_{\|b}(t)}{R_{\|b}(t)}\right]^2\right)\left.\right\}\left\{r^2\left[\frac{\dot R_{\perp a}(t)}{R_{\perp a}(t)}-\frac{\dot R_{\perp b}(t)}{R_{\perp b}(t)}\right]^2\right. \tag{10}$$
$$\left.+\frac{r^2}{4}\left[\Omega_a\left(\frac{R_{\perp 0}^2}{R_{\perp a}^2}-1\right)-\Omega_b\left(\frac{R_{\perp 0}^2}{R_{\perp b}^2}-1\right)\right]^2+x^2\left[\frac{\dot R_{\|a}(t)}{R_{\|a}(t)}-\frac{\dot R_{\|b}(t)}{R_{\|b}(t)}\right]^2\right\}^{1/2}4\pi r dr.$$

Note that (10) does not vanish even in the absence of the longitudinal and transverse cluster expansion ($\dot R_{\perp a,\perp b}(t) = \dot R_{\|a,\|b}(t) = 0$ because of the azimuthal $v_{\varphi a,\varphi b}$ revolution of ions in the magnetic field.

The magnetic field slows down the velocities $\dot R_{\perp a,\perp b}(t)$ of the transverse cluster expansion, therefore in (13) $r\dot R_{\perp a,\perp b}(t)$, $r\Omega_{a,\,b}R_{\perp a,\,\perp b}(t) \ll x\dot R_{\|a,\|b}(t)$ when the initial shape of the cluster is close to the spherical one, $R_{\|0} \sim R_{\perp 0} \sim R_0$. Disregarding the velocities $\dot R_{\perp a,\perp b}(t)$, $\Omega_{a,\,b}\,R_{\perp a,\,\perp b}(t) \sim \dot R_{\perp a,\perp b}(t)$ (due to the condition $\dot R_{\perp a,\perp b}/R_{\perp 0} \ll \dot R_{\|a,\|b}/R_{\|0}$), the formula (10) takes a simpler form:

$$N \approx \frac{9N_aN_b}{19\pi}\int_0^\infty dt\,\frac{1}{R_{\|b}^3(t)}\left(\frac{R_{\|b}^2(t)}{R_{\perp b}^2(t)}\right)\sigma_{ab}\left\{\frac{m_{ab}}{4}\left[\dot R_{\|a}(t)-\dot R_{\|b}(t)\frac{R_{\|a}(t)}{R_{\|b}(t)}\right]^2\right\}\left[\dot R_{\|a}(t)-\dot R_{\|b}(t)\frac{R_{\|a}(t)}{R_{\|b}(t)}\right]. \tag{11}$$

The comparison of (11) with (3) shows the following features: 1) with the magnetic field off when $R_{\|a,\,\|b}(t) = R_{\perp a,\,\perp b}(t) = R_{a,\,b}(t)$, the formula (11) turns into (3); 2) the functions $R_{\|a,\,\|b}(t)$ in (10) are similar to the functions $R_{a,\,b}(t)$ in (3); and 3) the dimensionless bracket specially highlighted in (11) is $(R_{\|b}^2(t)/R_{\perp b}^2(t)) \geq 1$ and so the time integral in (11) is larger than the integral in (3). Given these features of (11) and (3), we get an expression for the coefficient of enhancing the yield of reaction products due to the deceleration of expansion by the magnetic field as follows:

$$\frac{N_{\Omega\neq 0}}{N_{\Omega=0}} = \int_0^\infty dt \frac{1}{R_{\|b}^3(t)}\left(\frac{R_{\|b}^2(t)}{R_{\perp b}^2(t)}\right)\sigma_{ab}\left\{\frac{m_{ab}}{4}\left[\dot{R}_{\|a}(t) - \dot{R}_{\|b}(t)\frac{R_{\|a}(t)}{R_{\|b}(t)}\right]^2\right\}$$

$$\times\left[\dot{R}_{\|a}(t) - \dot{R}_{\|b}(t)\frac{R_{\|a}(t)}{R_{\|b}(t)}\right] \tag{12}$$

$$\times\left\{\int_0^\infty dt \frac{1}{R_b^3(t)}\sigma_{ab}\left\{\frac{m_{ab}}{4}\left[\dot{R}_a(t) - \dot{R}_b(t)\frac{R_a(t)}{R_b(t)}\right]^2\right\}\left[\dot{R}_a(t) - \dot{R}_b(t)\frac{R_a(t)}{R_b(t)}\right]\right\}^{-1}.$$

It is shown in [5] that the maximum magnetic fields causing magnetic compression of the central region of the cluster are generated at the maximum possible laser intensities. According to estimates and numerical calculations carried out in [6], for the intensity $I_{las} \approx 1 \times 10^{22}$ W/cm^2, the intrinsic magnetic field of the cluster with radius $R_0 = 300$ nm reaches 10 GG. With this laser intensity, the deuteron velocity (6) $c_{sb} = 6 \times 10^9$ cm/s, the dimensionless parameter $\beta = R_0^2\Omega_b^2/c_{sb}^2 \sim 0.06$ and then the equations (A1.2) can be solved by perturbation theory in the form of expansion in β. As a result:

$$R_{\|b} \approx \sqrt{R_0^2 + c_{sb}^2 t^2}, \quad R_{\perp b} \approx \sqrt{R_0^2(1 - 3\Omega_b^2 t^2/8) + c_{sa,sb}^2 t^2},$$

and substitution $R_{\|b}(t)$, $R_{\perp b}(t)$ in (12) leads to the following estimate:

$$\frac{N_{\Omega\neq 0}}{N_{\Omega=0}} \approx 1 + \frac{5R_0^2\Omega_b^2}{32c_{sb}^2}\frac{(2\chi^2 + 3\chi - 5)(\chi + 4)}{(\chi^2 + \chi - 2)(\chi + 6)}. \tag{13}$$

Thus, for a single cluster of spherical shape, the yield of reaction products increases little since deuterons with the energy required for the reaction in the intrinsic magnetic field of the cluster have a gyroradius $c_{sb}/\Omega_b \approx 1.5$ μm larger than the initial radius of the R_0 cluster. The increase in the yield according to (13) is ~6% for $\beta = 0.1$ and $\chi = 1.1$. Similarly, the contribution of N_{in} in (9) also increases.

The cluster magnetic field is insufficient to confine the bulk of the plasma volume of an individual cluster at a scale comparable to the cluster radius (reaching $\beta \sim 1$), but we can consider the confinement by the space-averaged magnetic field of the entire focal volume of the laser pulse and increase the N_{out} contribution. This confinement is reasonable only if the deuteron free path in the cluster plasma is much larger than the laser beam focus diameter D. The deuteron energy loss is caused mainly by DD collisions (the lightest ionic component). The free path length of the deuteron with respect to such collisions is described by the Bethe-Bloch formula:

$$l_{DD}(\varepsilon_D, \langle n_D\rangle) \approx (5.5\times 10^{-2}\ \text{cm})(10^{22}\ \text{cm}^{-3}/\langle n_D\rangle)(\varepsilon_D/10\ \text{MeV})^2,$$

where $\langle n_D\rangle$ is the average concentration of deuterium nuclei in the focal volume. We assume that the condition $D \ll l_{DD}(\varepsilon_D, \langle n_D\rangle)$ is satisfied since it can be violated with the focal region diameters of the order of hundreds of micrometers, which corresponds to a very high (hundreds of J) laser pulse energy.

Modern frequency lasers capable of repeating a pulse with frequency in units of Hz have characteristic pulse energy of the order of J units, and when the frequency is hundreds of Hz, the pulse energy is in tens of mJ. In this case, $D \leq 30\ \mu\text{m} \ll l_{DD}(\varepsilon_D, \langle n_D\rangle)$ in the range of laser intensities discussed here. The yield of nuclear reactions for such lasers will be reduced due to the escape of deuterons from the focal volume, but the latter can be magnetized by switching from the linear to circular polarization of the laser pulse, which will increase the effective path length of the accelerated deuteron in the plasma and, consequently, the reaction yield. Let us estimate the magnetic field required for magnetization of the focal volume. It is shown in [5] that the magnetic field of a single cluster is estimated at the end of the laser pulse as

$$\frac{H(\tau_{las})}{E_{las}} \approx \frac{\eta a_0 c\tau_{las}}{16R_0(1 + a_0^2)^{1/2}},$$

($a_0 = [I_{las}\lambda^2/(1.37 \times 10^{18}\ \text{W}\,\mu\text{m}^2/\text{cm}^2)]^{1/2}$, η is the cluster absorption coefficient), and Appendix 2 shows the law of diminishing cluster magnetic field after the end of the laser pulse: $H(t)/H(\tau_{las})$, $t > \tau_{las}$

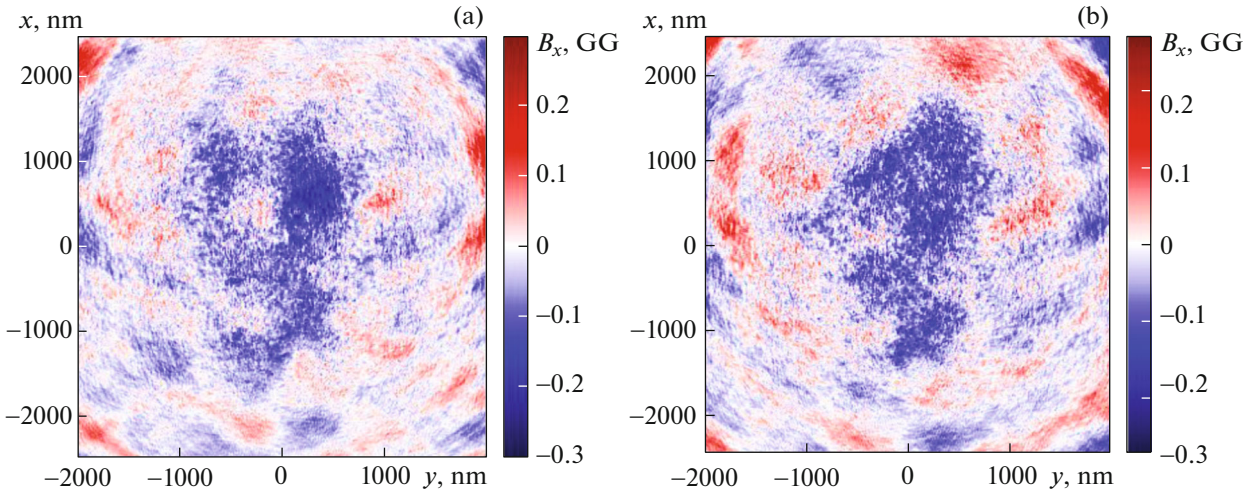

Fig. 3. Spatial distribution of the magnetic field in the focal volume of laser pulse.

(see (A2.1)). The time dependence of the magnetic field can be expressed by combining these estimates through the time dependence of the cluster radius:

$$H(t) \approx E_{\text{las}} \frac{\eta a_0 c \tau_{\text{las}}}{16 R_0 (1 + a_0^2)^{1/2}} \frac{R_0^3 \gamma(\tau_{\text{las}})}{R^3(t)\{1 + [\gamma(\tau_{\text{las}}) - 1][R_0/R(t)]^2\}}. \tag{14}$$

In the case of strongly relativistic electrons ($\gamma(\tau_{\text{las}}) \gg 1$) $H(t) \sim R^{-1}(t)$ and for weakly relativistic electrons $H(t) \sim R^{-3}(t)$ [5].

Thus, the clusters expanded to the maximum distance s form a quasi-uniform laser plasma in the focal volume with a volume-averaged magnetic field:

$$\langle H \rangle = \frac{R_0}{s} H, \quad \langle \Omega_b \rangle = \frac{R_0}{s} \Omega_b. \tag{15}$$

The spatial distribution of the magnetic field in the focal volume of the laser pulse for numerical PIC simulation of the laser cluster plasma is shown in Fig. 3. The average field in the focal volume is ~0.1 GG, which corresponds to the estimate (15).

To prevent the cluster plasma of the focal volume from expanding in the transverse direction, it is necessary to satisfy the condition $2c_{\text{sb}}/(D\langle\Omega_b\rangle) < 1$. This condition (the condition of magnetization of the focal volume) expressed through the parameters of the laser pulse and the parameters of the clusters has the form:

$$\frac{D}{\lambda}\left(\frac{I\lambda^2}{1.37 \times 10^{18}\ \text{W}\,\mu\text{m}^2/\text{cm}^2}\right)^{(1-\mu)/2} > \frac{s}{\pi R_0}\sqrt{\frac{m_b}{Z_b m_e}}. \tag{16}$$

We introduce the "critical" focus diameter

$$D_{\text{cr}} = \frac{\lambda s}{\pi R_0}\sqrt{\frac{m_b}{Z_b m_e}}\left(\frac{I\lambda^2}{1.37 \times 10^{18}\ \text{W}\,\mu\text{m}^2/\text{cm}^2}\right)^{(\mu-1)/2},$$

corresponding to the lower boundary of the inequality (16). For $\mu \approx 0.75$, the relationship $D_{\text{cr}}(I)$ becomes weak: $D_{\text{cr}}(I) \sim I^{-0.13}$. The "critical" diameter can be considered with accuracy up to a multiplier ~1 to be independent of intensity: $D_{\text{cr}}(I) = \text{const}(I)$. We get $D_{\text{cr}} \approx 40$ μm and the 30-femtosecond laser pulse energy of around 40 J for the intensity $I = 10^{20}$ W/cm^2, which is available nowadays for experiments. The laser with such pulse characteristics can operate with repetition frequency in units of Hz [8]. The expansion of the focal volume under condition (16) will occur only in the longitudinal direction with the characteristic expansion time $\tau_{\parallel} \approx \pi D^2/(4\lambda c_{\text{sb}})$ (it is this time that will determine the reaction yield in contrast to the

time D/c_s in the nonmagnetized case), provided that the energy loss on collisions is small, for which the characteristic time of energy loss is

$$\tau_c \approx \frac{m_b c_{sb}^3}{Z_a^2 e^2 \langle \omega_{pe} \rangle^2 \ln\Lambda},$$

where $\langle \omega_{pe} \rangle$ is determined by the average electron density of the focal volume and $\ln\Lambda$ is the Coulomb logarithm. Since the parameter $\chi \approx 1.1$ for the reaction Li(D, n) ^{8}Be, the magnetization condition in the focal volume of deuterium ions coincides with that for lithium ions. Considering also that the distance s between clusters depends on the concentration of clusters n_{cl} in the focal volume with $s = n_{cl}^{-1/3}$, the condition (16) can be written as an inequality for the density of clusters required for magnetic confinement in the form:

$$n_{cl} > \left[\frac{\lambda}{\pi R_0 D} \sqrt{\frac{m_b}{Z_b m_e}} \left(\frac{I\lambda^2}{1.37\times10^{18}\ \mathrm{W\,\mu m^2/cm^2}} \right)^{(\mu-1)/2} \right]^3 = n_{cl}^*. \tag{17}$$

Estimates of the increase in the yield of nuclear reactions imply that the focal volume of the laser pulse is located inside the cluster jet, so its diameter should exceed the focal length, and the laser pulse absorption length should be comparable to the focal length. The focal length is close to 1 mm for $D_{cr} \approx 40$ μm. The real cluster jet flying out of a nozzle of the required diameter has an angular divergence of ~30°, which leads to the formation of an area of density inhomogeneity at distances of the order of the jet diameter with a characteristic scale of hundreds of micrometers. If the laser pulse is absorbed on the periphery of the gas-cluster jet in the region of cluster concentrations that do not satisfy inequality (17), the magnetic field will not affect the reaction yield. The laser pulse absorption length in the cluster plasma was discussed in [21] and it is

$$l_{ph} \approx \left(\frac{I\lambda^2}{1.37\times10^{18}\ \mathrm{W\,\mu m^2/cm^2}} \right)^{1/2} \frac{c\tau_{las} n_{ec}}{4\langle n_e \rangle}, \tag{18}$$

where $n_{ec} = m_e\omega^2/(4\pi e^2)$ and $\langle n_e \rangle \approx (4\pi/3) Z n_{i0} R_0^3 n_{cl}$ are the critical and volume-averaged electron concentrations in the plasma, respectively. For the laser radiation to be able to reach the gas jet density regions satisfying inequality (17), the obvious condition should be satisfied for the scale of inhomogeneity, δl, of the radial distribution of cluster concentrations, $n_{cl}(l)$:

$$\delta l < \left(\frac{I\lambda^2}{1.37\times10^{18}\ \mathrm{W\,\mu m^2/cm^2}} \right)^{1/2} \frac{3c\tau_{las} n_{ec}}{16\pi Z n_{i0} R_0^3 n_{cl}^*}. \tag{19}$$

We get $l_{ph} \approx 400$ μm for a cluster with radius 100 nm and concentration $n_{cl}^* \approx 1$ μm^{-3}, laser intensity of 10^{21} W/cm^2, and laser pulse duration of 30 fs, which is comparable to the Rayleigh length and the scale of inhomogeneity (nozzle diameter) of the cluster jet. Note that for lower laser intensities (10^{19} to 10^{20} W/cm^2) and short absorption lengths l_{ph}, inequality (19) can be broken and then the magnetic field will not affect the yield of nuclear reactions, and the number of reaction products will be determined by formula (8) with the number of clusters in the absorption length volume instead of the focal length volume.

In order to find the yield of reaction products from the entire magnetized focal volume, we can use formula (11) taking into account that the total number of ions of each type in the focal volume is $N_{cl} N_{a,\,b}$, the size of the focal volume $R_{\perp b} \approx c_{sb}/\langle \Omega_b \rangle$, $R_{\parallel b} \approx \pi D^2/(4\lambda)$. As a result, the estimate of the yield of reaction products under conditions (16), (17) take the form

$$N_{out} \approx \frac{N_a N_b N_{cl}^2 \langle \Omega_b \rangle^2}{8\pi c_{sb}^2} \sigma_{ab} \left(W \left(\sqrt{\frac{Z_b m_{ab}}{m_b}} - \sqrt{\frac{Z_a m_{ab}}{m_a}} \right)^2 \right), \tag{20}$$
$$\tau_\parallel < \tau_c, \quad N_{tot} = N_{in} + N_{out}.$$

The comparison of the yield of reaction products, N_{out}, in the absence of the magnetic field (7) and N_{out} in the presence of the field (20) shows that the yield of intercluster reactions increases approximately

by $\langle\Omega_b\rangle^2 D^3/(\lambda c_{sb}^2)$ times. This factor has a simple explanation: when the field is absent, the characteristic time of reactions in the focal volume is equal to D/c_{sb}, then the density and energy of particles drop. The magnetic field stops the transverse expansion, increases the density by $\langle\Omega_b\rangle^2 D^2(4c_{sb}^2)^{-1}$ times, and the characteristic time of reactions becomes $\pi D^2/(4\lambda c_{sb})$. It is the increased density and reaction time that lead to the factor $\langle\Omega_b\rangle^2 D^3/(\lambda c_{sb}^2)$. In the presence of strong absorption ($l_{ph} < \pi D^2/(4\lambda)$), the absolute yield of neutrons will decrease, in which case the number of clusters, N_{cl}, in the absorption volume $\pi D^2 l_{ph}/4$ instead of the focal volume $\pi^2 D^4/(16\lambda)$ will be included in the estimate (20). The enhancement in the neutron yield at the expense of the magnetic field will remain (if conditions (16), (17) are satisfied), but the enhancement factor will be smaller being $\langle\Omega_b\rangle^2 D l_{ph}/c_{sb}^2$ instead of $\langle\Omega_b\rangle^2 D^3/(\lambda c_{sb}^2)$ at weak absorption. Numerically estimate the neutron yield and the parameters of the laser pulse and the cluster plasma, which enhance the neutron yield due to the confinement of the laser plasma by the magnetic field. The number of particles in one cluster $N_{Li,\ D} \approx 10^9$ with an ion concentration of 10^{22} cm^{-3} for the cluster radius $R_0 = 300$ nm. When the intensity of the 10-femtosecond laser pulse is 10^{22} W/cm^2, $D_{cr} \approx 20$ μm, $c_{sb}/\Omega_b \approx 8$ μm, and $N_{cl} \approx 3000$. The yield N_{tot} (20) will be ~8×10^6 neutrons for $\sigma_{ab} \approx 1$ barn. Calculation by formula (7) without a magnetic field (linear laser pulse polarization) with the same parameters of the clusters gives 2×10^5 neutrons. Thus, changing the polarization of the laser pulse and taking into account the generated magnetic field make it possible to increase the yield of reaction products by a factor of about 40. Figure 4 shows the dependence of N_{tot} on the laser intensity of a 10-femtosecond pulse (blue curve) based on the formula (20) for clusters with radius $R_0 = 300$ nm, $s = 4R_0$ for the laser spot diameter $D_{cr}(I)$ corresponding to the boundary of (16), the neutron yield being also shown in the absence of a magnetic field (8) for clusters with radius $R_0 = 100$ nm (black curve) and $R_0 = 300$ nm (red curve). It can be seen that the magnetization of the focal volume enhances the neutron yield over the entire range of laser intensities sufficient for initiating nuclear reactions. A yield of ~10^7 neutrons per 1 J of laser energy was achieved under the condition $l_{DD}(\varepsilon_D, n_D) < D$ in numerical simulation [22] with optimization of deuterium cluster plasma and a laser intensity of 3×10^{19} W/cm^2 for a 30-femtosecond, linearly polarized laser pulse. The implementation of such a yield requires sufficiently large values of the laser pulse diameter D, of the focal volume, and of laser pulse energy. It was shown in [23] that the laser pulse energy should be hundreds of J to achieve this neutron yield. In the case of the opposite condition, $D < \pi D^2/(4\lambda) < l_{DD}(\varepsilon_D, n_D)$, corresponding to a low laser energy, the neutron yield will drop by about a factor of $\pi D^4/(4\lambda l_{DD}^3(\varepsilon_D, n_D))$ and it will be ~10^4 neutrons/J for a laser pulse of the same duration and intensity with a focus diameter of ~10 μm. A yield of 6×10^4 neutrons/J was experimentally achieved in [24].

Note that the use of high laser intensities and pulse energies in the estimates of this paper is aimed at obtaining the maximum neutron yield per 1 J of laser energy. If you do not set this task but limit yourselves to a basic demonstration of the effect of neutron yield enhancement by generating a magnetic field with a circularly polarized laser pulse, the range of laser parameters expands. The pulse duration should not exceed the expansion time of a single cluster, which corresponds to tens of femtoseconds. The laser intensity is basically limited from below by deuteron energy (~1 MeV) required for the Li–D nuclear reaction; it is of the order of 10^{19} W/cm^3. The focus diameter and density of clusters in the jet should satisfy the inequality (17). For a density of 1 cluster/μm^3, the focus diameter satisfying (17) will be ~70 μm, which is less than the free path of a deuteron. Thus, the implementation of the effect of magnetic confinement of the focal plasma volume (of a relative increase in neutron yield when circular polarization is used instead of linear polarization) is possible for a laser pulse with an intensity higher than 10^{19} W/cm^3, duration of up to 40 fs, and the spot diameter of 70 μm. When the spot diameter is in the range from 70 μm to the scale of the deuteron free path length (~300 μm), the use of circular polarization will increase the neutron yield.

Thus, at laser pulse energies in units and tens of joules, the use of circularly polarized laser pulse with high intensity and of the magnetic field generated by this pulse can significantly increase the yield of nuclear reactions in cluster laser plasma compared to the use of linearly polarized laser pulse. Note also that lasers with energies in units of joules or less are capable of operating in the frequency mode (with a frequency of ~1 kHz) of pulse generation [19]. Accordingly, the lower specific neutron yield per 1 J of laser energy when using circular polarization and magnetic field (~10^6 neutrons/J) compared to a laser pulse with linear polarization and energy of hundreds of J (~10^7 neutrons/J) can be exceeded when switching to the generation mode with a pulse repetition rate of hundreds of Hz or higher.

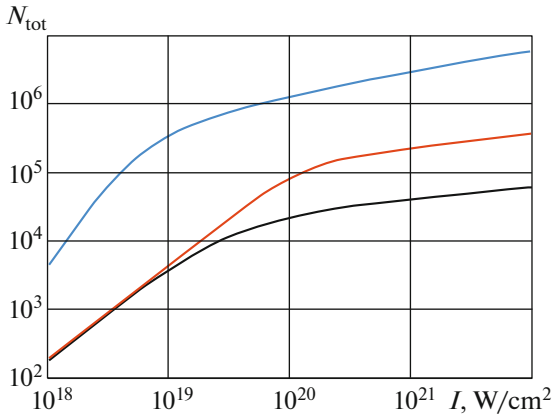

Fig. 4. The dependence of the neutron yield N_{tot} (17) on the laser pulse intensity (τ_{las} = 10 fs) for clusters with the radius R_0 = 300 nm, $s = 4R_0$, $D(I)$ when the magnetic field is taken into account (blue curve), and the dependence of the neutron yield (7) in the absence of a magnetic field on the laser intensity of a 10 femtosecond pulse for clusters with radii R_0 = 100 nm (black curve) and 300 nm (red curve), D = 10 μm, $s = 4R_0$.

4. CONCLUSIONS

This paper shows that a relativistically intense circularly polarized laser pulse interacting with a cluster laser plasma generates a space-averaged magnetic field sufficient to keep the focal volume of the plasma from transverse expansion. An extension of the plasma lifetime (confinement time) increases the yield of intercluster nuclear reactions arising from collisions of plasma ions when the laser pulse focus diameter is smaller than the free path length of ions accelerated in the laser plasma. This condition is satisfied for lasers with small pulse energy, but it is violated starting from energies of hundreds of joules. Lasers with pulse energies in units of joules are capable of operating in the pulse repetition mode with a frequency from units of Hz and the cluster target in this case will make it possible to create a quasi-stationary neutron source. The neutron yield can be increased tens of times with the reaction of neutron production Li + D = ^{8}Be + n (clusters in the form of LiF salt solution in heavy water) and laser energy in units of joules. So, the neutron yield achieved in experiments on heating cluster plasma with a linearly polarized pulse of low energy can be significantly increased by switching from linear to circular polarization of the laser pulse.

APPENDIX 1

Reference [12] presents equations that describe the dynamics of adiabatic thermal expansion (adiabatic exponent 5/3) of an elliptical ion cluster (semiaxis lengths $X_{a,b}(t)$, $Y_{a,b}(t)$, $Z_{a,b}(t)$) in the magnetic field H:

$$\ddot{Y}_{a,b} + \Omega_{a,b}\dot{Z}_{a,b} = -\frac{\partial U_{a,b}}{\partial Y_{a,b}},$$

$$\ddot{Z}_{a,b} - \Omega_{a,b}\dot{Y}_{a,b} = -\frac{\partial U_{a,b}}{\partial Z_{a,b}}, \quad \ddot{X}_{a,b} = -\frac{\partial U_{a,b}}{\partial X_{a,b}},$$

$$U_{a,b} = \frac{(5\mu - 3)c_{sa,sb}^2}{\mu - 1}\left[\frac{X_{a,b}(0)Y_{a,b}(0)Z_{a,b}(0)}{X_{a,b}(t)Y_{a,b}(t)Z_{a,b}(t)}\right]^{\mu-1}, \qquad \text{(A.1.1)}$$

$$\Omega_{a,b} = \frac{Z_{a,b}eH}{m_{a,b}c}.$$

The characteristic thermal velocities of ions, $c_{sa,sb}$ are determined by (6) with the parameter $k = 0$.

When the magnetic field in (A1.1) is switched off, $X_{a,b}(t) = Y_{a,b}(t) = Z_{a,b}(t) = R_{a,b}(t)$ and the effective potential energy responsible for thermal expansion is $U_{a,b} \sim R_{a,b}^{-2}$ according to the same summand in the

law of conservation of energy (4). The equations (A1.1) in this case have solution (6) with the parameter $k = 0$. There is a motion integral $P_{\varphi a,\,\varphi b} = R^2_{\perp a,\perp b}(\dot{\varphi}_{a,b} + \Omega_{a,\,b}) = \text{const}$ when the magnetic field is taken into account for a cluster in the form of an ellipsoid of revolution $X_{a,b}(t) = R_{\parallel a,\,\parallel b}(t) \neq Y_{a,b}(t) = Z_{a,b}(t) = R_{\perp a,\,\perp b}(t)$ (i.e., azimuthal-symmetric expansion) in the system (A1.1), which allows obtaining a set of equations for the semiaxes of the ellipsoid of revolution $R_{\parallel a,\,\parallel b}(t)$, $R_{\perp a,\,\perp b}(t)$:

$$\ddot{R}_{\parallel a,\parallel b} = -\frac{\partial U_{a,b}}{\partial R_{\parallel a,\parallel b}} = \frac{16c^2_{\text{sa,sb}}}{3R_{\parallel a,\parallel b}}\left(\frac{R_{\parallel 0}R^2_{\perp 0}}{R_{\parallel a,\parallel b}R^2_{\perp a,\perp b}}\right)^{2/3},$$

$$\ddot{R}_{\perp a,\perp b} = -\frac{\partial U^{\text{eff}}_{a,b}}{\partial R_{\perp a,\perp b}} = \frac{16c^2_{\text{sa,sb}}}{3R_{\perp a,\perp b}}\left(\frac{R_{\parallel 0}R^2_{\perp 0}}{R_{\parallel a,\parallel b}R^3_{\perp a,\perp b}}\right)^{2/3}$$

$$-\frac{\Omega^2_{a,b}R_{\perp a,\perp b}}{4}\left(1 - \frac{R^4_{\perp 0}}{R^4_{\perp a,\perp b}}\right), \tag{A.1.2}$$

$$U_{a,b} = 8c^2_{\text{sa,sb}}\left(\frac{R_{\parallel 0}R^2_{\perp 0}}{R_{\parallel a,\parallel b}R^2_{\perp a,\perp b}}\right)^{2/3},$$

$$U^{\text{eff}}_{a,b} = U_{a,b} + \frac{\Omega^2_{a,b}R^2_{\perp a,\perp b}}{8}\left(1 + \frac{R^4_{\perp 0}}{R^4_{\perp a,\perp b}}\right).$$

Here $R_{\parallel 0}$, $R_{\perp 0}$ are the lengths of semiaxes of the ellipsoid at the initial moment of time.

It can be seen from the system (A1.2) that the magnetic field leads to the appearance of the effective potential energy $U^{\text{eff}}_{a,b}$ of expansion in the transverse direction, which has the form of a potential well with respect to $R_{\perp a,\,\perp b}$. The presence of the well stops the expansion along the transverse coordinate $R_{\perp a,\,\perp b}$ at the scales of ion gyroradii. The expansion does not stop along the longitudinal coordinate but the expansion acceleration changes: $\ddot{R}_{\parallel a,\parallel b} \sim R^{-5/3}_{\parallel a,\parallel b}$ unlike $\ddot{R}_{a,b} \sim R^{-3}_{a,b}$ without the magnetic field in the spherically symmetric case. The solutions to the system (A1.2) always satisfy the inequality $R_{\perp a,\,\perp b}(t) \leq R_{\parallel a,\,\parallel b}(t)$ because of the presence of an additional inhibitory force in the transverse direction. Moreover, the motion of ions of two types is finite in the transverse direction and they continue to collide revolving in the magnetic field in the space bounded in the transverse direction. The gyroradii of the ions $c_{\text{sa, sb}}/\Omega_{\text{sa, sb}}$ should not exceed the focal waist radius $D/2$ (the transverse size of the area occupied by the magnetic field) for the transverse motion to be finite.

The ion densities and velocities take the following form for estimating the yields of the reaction products (1) at anisotropic expansion in the longitudinal and transverse directions:

$$n_{a,b}(r,t) = \frac{\theta(R_{a,b}(t) - r)N_{a,b}}{\pi R_{\parallel a,\parallel b}R^2_{\perp a,\perp b}(t)}, \quad v_{\perp a,\perp b}(r,t) = \frac{r_\perp \dot{R}_{\perp a,\perp b}(t)}{R_{\perp a,\perp b}(t)},$$

$$v_{\parallel a,\parallel b}(r,t) = \frac{x\dot{R}_{\parallel a,\parallel b}(t)}{R_{\parallel a,\parallel b}(t)}, \quad v_{\varphi a,\varphi b} = r\dot{\varphi}_{a,b} = \frac{r\Omega_{a,b}(R^2_{\perp 0}/R^2_{\perp a,\perp b} - 1)}{2}. \tag{A.1.3}$$

APPENDIX 2

The magnetic field of an individual cluster [5]

$$H \approx E_{\text{las}}\frac{\eta a_0 c\tau_{\text{las}}}{16R_0(1 + a_0^2)^{1/2}} \sim E_{\text{las}}.$$

After the end of the laser pulse, the electron momentum remains and is an adiabatic invariant unaffected by the slow change of the cluster parameters. The orbital magnetic moment of the electron is related to its mechanical momentum through the gyromagnetic ratio, which is equal to $e/(2m_e c\gamma(t))$ for a relativistic electron, where $\gamma(t)$ is the Lorentz factor of the electron at a fixed moment of time. The magnetic field of the revolving and expanding cluster shell is determined by the magnetic moment of the unit volume,

in which the concentration of electrons, $n_e(t)$ also falls as they expand. We get as a result the following dependence of the magnetic field on time after the end of the laser pulse:

$$H(t) \approx H(\tau_{las})\frac{n_e(t)\gamma(\tau_{las})}{n_e(\tau_{las})\gamma(t)}, \quad \tau > \tau_{las}.$$

In adiabatic expansion, the electron concentration and Lorentz factor depend obviously on the cluster radius as follows:

$$\frac{n_e(t)}{n_e(0)} = \frac{R_0^3}{R^3(t)}, \quad \gamma(t) = 1 + [\gamma(\tau_{las}) - 1]\left(\frac{R_0}{R(t)}\right)^2.$$

The following estimate results for the time dynamics of the magnetic field after the end of the laser pulse:

$$H(t) \approx H(\tau_{las})\left(\frac{R_0^3\gamma(\tau_{las})}{R^3(t)\{1 + [\gamma(\tau_{las}) - 1][R_0/R(t)]^2\}}\right), \quad t > \tau_{las}. \tag{A.2.1}$$

ACKNOWLEDGMENTS

The authors are grateful to the Polytechnic-RSC Tornado computer center for the provided computing resources.

FUNDING

The study was supported by the Russian Science Foundation (grant no. 23-22-00110).

CONFLICT OF INTEREST

The authors declare that they have no conflicts of interest.

REFERENCES

1. Krainov, V.P. and Smirnov, M.B., *Phys. Rep.,* 2002, vol. 370, p. 237.
2. Zweiback, J., Smith, R.A., Cowan, T.E., Hays, G., Wharton, K.B., Yanovsky, V.P., and Ditmire, T., *Phys. Rev. Lett.,* 2000, vol. 84, p. 2634.
3. Peano, F., Fonseca, R.A., Martins, J.L., and Silva, L.O., *Phys. Rev. A*, 2006, vol. 73, p. 053202.
4. Last, I. and Jortner, J., *Phys. Rev. A,* 2008, vol. 77, p. 033201.
5. Lecz, Zs. and Andreev, A., *Phys. Rev. Res.,* 2020, vol. 2, p. 023088.
6. Andreev, A.A. and Platonov, K.Yu., *Quantum Electron.,* 2021, vol. 51, p. 446.
7. Andreev, A.A., Platonov, K.Yu., et al., *Sci. Rep.,* 2021, vol. 11, p. 15971.
8. Nagymihaly, R.S., Falcoz, F., Bussiere, B., Bohus, J., Pajer, V., Lehotai, L., Ravet-Senkans, M., Roy, O., Calvez, S., Mollica, F., Branly, S., Paul, P.-M., Börzsönyi, Á., et al., *Opt. Express,* 2023, vol. 31, p. 44160.
9. Bychenkov, V.Yu., Tikhonchuk, V.T., and Tolokonnikov, S.V., *JETP,* 1999, vol. 88, p. 1137.
10. Ditmire, T., Donnelly, T., Rubenchik, A.M., Falcone, R.W., and Perry, M.D., *Phys. Rev. A,* 1996, vol. 53, p. 3379.
11. Bychenkov, V.Yu. and Kovalev, V.F., *Plasma Phys. Rep.,* 2005, vol. 31, p. 178.
12. Anisimov, S. and Lysikov, Yu., *J. Appl. Math. Mech.,* 1970, vol. 34, p. 882.
13. Srivastava, M.K., Sinha, B.K., and Lawande, S.W., *Phys. Fluids,* 1988, vol. 31, p. 394.
14. Bychenkov, V.Yu. and Kovalev, V.F., *JETP,* vol. 101, no. 2, p. 212.
15. Kemp, A.J. and Ruhl, H., *Phys. Plasmas,* 2005, vol. 12, p. 033105.
16. Gozhev, D.A., Bochkarev, S.G., and Bychenkov, V.Yu., *JETP Lett.,* 2021, vol. 114, no. 4, p. 200.
17. Wilks, S.C., Langdon, A.B., Cowan, T.E., Roth, M., Singh, M., Hatchett, S., Key, M.H., Pennington, D., et al., *Phys. Plasmas,* 2001, vol. 8, p. 542.
18. Davis, J. and Petrov, G.M., *Phys. Plasmas,* 2011, vol. 18, p. 073109.

19. Knight, B., Gautam, C., Stoner, C., Egner, B., Smith, J., Orban, C., and Manfredi, J., *High Power Laser Sci. Eng.,* 2024, vol. 12, p. e2.
20. EPOCH code repository. https://github.com/Warwick-Plasma/epoch.
21. Decker, C.D., Mori, W.B., Tzeng, K.C., and Katsouleas, T., *Phys. Plasmas,* 1996, vol. 3, p. 2047.
22. Bochkarev, S.G., Brantov, A.V., Gozhev, D.A., and Bychenkov, V.Yu., *J. Russ. Laser Res.,* 2021, vol. 42, p. 292.
23. Gozhev, D.A., Bochkarev, S.G., Lobok, M.G., et al., *Quantum Electron.,* 2023, vol. 53, p. 217.
24. Semenov, T.A., Gorlova, D.A., Dzhidzhoev, M.S., et al., *Laser Phys. Lett.,* 2022, vol. 19, p. 095401. https://doi.org/10.1088/1612-202X/ac7ecb

Translated by D. Sventsitsky